



ARTICLE

Effects of Biowaste-Derived Hydrochar on Anaerobic Digestion: Insights into Hydrochar Characteristics

Hongqiong Zhang^{1,2,#}, Xu Wang^{3,#}, Zhaojing Qian⁴, Buchun Si^{1,4,*}, Kai Jin⁵ and Tengfei Wang⁵

¹Key Laboratory of Agricultural Renewable Resource Utilization Technology, College of Engineering, Northeast Agriculture University, Harbin, 150030, China

²College of Engineering, Northeast Agricultural University, Harbin, 150030, China

³College of Food Science, Northeast Agricultural University, Harbin, 150030, China

⁴Laboratory of Environment-Enhancing Energy (E2E), Key Laboratory of Agricultural Engineering in Structure and Environment, Ministry of Agriculture, College of Water Resources and Civil Engineering, China Agricultural University, Beijing, 100083, China

⁵Faculty of Geosciences and Environmental Engineering, Southwest Jiao Tong University, Chengdu, 611756, China

*Corresponding Author: Buchun Si. Email: sibuchun@cau.edu.cn

#Those authors contribute equally

Received: 17 December 2022 Accepted: 13 February 2023 Published: 10 August 2023

ABSTRACT

Hydrochar prepared with four typical biowastes, pine wood, food waste, digested sewage sludge, and *Chlorella* were applied for the promotion of anaerobic digestion. The gas production and substrate composition were analyzed associated with the hydrochar characteristics. The results suggested that *Chlorella* hydrochar (C-C) showed the highest cumulative yield of methane (approximately 345 mL) with high total organic carbon (TOC) removal efficiency and low volatile fatty acids (VAFs) concentration. Especially, food waste hydrochar (F-C) showed a poor effect on anaerobic digestion and aroused 1.4–1.6 g/L accumulation of VAFs, in which the toxic components may account for the low efficiency. The C-C and sludge hydrochar (S-C) may develop direct interspecific electron transport (DIET) to facilitate the generation of methane by both surface groups and conductivity of the body structure, unlike pinewood hydrochar (P-C), which mainly depended on the aromatic matrix structure of hydrochar body. This work suggested that C-C can be the best candidate for the facilitation of anaerobic digestion, and N-containing biowaste like algae and lignocellulose like pine wood may establish different DIET pathways based on the physicochemical characteristics of hydrochar.

KEYWORDS

Biowaste; hydrochar; DIET; anaerobic digestion; methane

1 Introduction

With the depletion of traditional fossil energy and the continuous attenuation of environmental carrying capacity, biofuel has become one of the most important forms of energy to make up for the global energy shortage with low carbon emissions [1,2]. Exploring advanced green, renewable, and sustainable technologies of biowaste valorization have been a hot topic [3,4]. Over the last few decades, the production of methane from the anaerobic digestion of organic wastes is regarded as an elegant and



economical pathway for generating renewable biofuel [5]. However, one issue is that the anaerobic digestion is sensitive to the organic load and reaction environment [6,7]. Therefore, researchers have been trying to lessen the effects of these factors and improve the efficiency of anaerobic digestion [8].

Biogas production from anaerobic digestion through direct interspecific electron transport (DIET) has attracted increasing attention. Because the main process of anaerobic digestion methanogenesis is finished by indirect interspecific electron transport mediated by hydrogen and formic acid, the degradation of substrates by methanogenic archaea can be limited, which is directly related to the efficiency of electron transport [9,10]. Microbes could directly reduce CO₂ to methane using pili or C-type cytochrome electrons [11]. Research has been carried out on adding exogenous conductive materials to the system of anaerobic digestion, which is expected to bring high degradation efficiency. The microorganisms in anaerobic systems can complete the long-distance transfer of electrons between species without consuming cellular energy [12].

It reported that conductive materials such as graphene, carbon cloth, magnetite, biochar, and granular activated carbon could reduce the impact of the substrate fermentation environment and accelerate the transformation of volatile fatty acids (VAFs) [13–15]. For carbon-based materials, the theory of promoting electron transport through the material matrix and surface functional groups has been confirmed [16,17]. Several works showed that the electrical conductivity of the main carbon structure and the surface oxygen-containing functional groups (phenolic hydroxyl and quinone groups) could develop DIET [18,19]. Among these, hydrochar can be directly obtained from wet biowaste, which keeps enough oxygen-containing groups such as -OH and C=O on the surface, and the electrochemical properties make it an excellent candidate for the establishment of DIET [20–22].

However, current research on the application of different biowaste hydrochar in anaerobic digestion is still unknown, especially the difference between lignocellulose and nitrogen-containing biowaste-derived hydrochar. Since the nitrogen components in biowaste participate in carbonization, the properties and application of the generated hydrochar in anaerobic digestion is a mystery. Given this, this study intends to use typical lignocellulose and nitrogen-containing biowaste hydrochar as additives to promote the anaerobic process by developing DIET. The effects on syngas production and substrate composition were investigated in detail by comparing the differences between lignocellulosic hydrochar and nitrogen-containing biowaste hydrochar. This work would provide a theoretical basis for the application of hydrochar in promoting anaerobic digestion, and better application strategies can be expected to enhance the efficiency of anaerobic digestion.

2 Materials and Methods

2.1 Materials

Pinewood sawdust was selected as typical lignocellulose material to compare the effect of hydrochar from lignocellulose, and nitrogen-containing biowaste on the anaerobic digestion process nitrogen-containing biowastes including food waste, digested sewage sludge, and *Chlorella* were selected as nitrogen-rich feedstock. The proximate analysis of the feedstock is shown in Table 1. For each run of hydrothermal carbonization, a mass ratio of 85% (feedstock/water, close to the moisture) was prepared for the feedstock, meaning approximately 170 g water and 30 g dried biowaste was added, which was close to the natural moisture content of the feedstock. The reactor was heated at a rate of 5°C/min, and a final residence temperature was set as 250°C. After hydrothermal carbonization, the reactor was cooled to room temperature, and the mixture was separated by vacuum filtration. The solid residue, food waste hydrochar (F-C), *Chlorella* hydrochar (C-C), sludge hydrochar (S-C), and pinewood hydrochar (P-C) with certain moisture were further dried in an oven at 105°C until a constant mass was reached. After grinding, all the hydrochar samples were used to pass through a 40-mesh (0.63 mm) sieve.

Table 1: Proximate analysis of the feedstock

Feedstock	Proximate analysis (% wt.)		
	Volatile	Ash	Fixed carbon
Pine	89.57	4.91	5.52
Food waste	91.18	5.51	3.31
Sludge	42.50	56.05	1.45
<i>Chlorella vulgaris</i>	85.39	3.93	10.68

2.2 Methods

Hydrochar was used as an additive during anaerobic digestion, and the amount of hydrochar was set as 2.5 g/L. To mimic the anaerobic digestion, synthetic wastewater was used as the substrate. The COD concentration of synthetic wastewater was set at 5 g/L. The granular anaerobic sludge was used for inoculum with a volume of 40 mL. For comparison, the anaerobic digestion without hydrochar addition was set as the control group. Anaerobic digestion was conducted using an automatic methane potential test system-II (AMPTS II, Bioprocess Control AB, Lund, Sweden). The total working volume was 400 mL and with 200 mL headspace. The liquid samples were taken every day, and total organic carbon (TOC) and low VAFs concentrations were measured. Each bottle was fed with 400 μ L nutrient stock solution, and each liter of nutrient stock solution contained 0.48 g $\text{CoCl}_2 \cdot 6\text{H}_2\text{O}$, 0.1 g $\text{CuCl}_2 \cdot 2\text{H}_2\text{O}$, 1.3 g ZnCl_2 , 5 g $\text{MnCl}_2 \cdot 4\text{H}_2\text{O}$, 2.5 g $\text{FeCl}_3 \cdot 6\text{H}_2\text{O}$, 0.4 g $\text{NiSO}_4 \cdot 6\text{H}_2\text{O}$, 0.1 g $\text{AlK}(\text{SO}_4)_2 \cdot 12\text{H}_2\text{O}$, 0.25 g $\text{Na}_2\text{MoO}_4 \cdot 2\text{H}_2\text{O}$.

The TOC of aqueous samples was measured by a TOC analyzer equipped with a Nondispersive infrared (NDIR) gas detector (TOC-V CPN, Shimadzu, Japan). The VFAs were analyzed through gas chromatography (Shimadzu Nexis-2030, Japan) which was equipped with a flame ionization detector (FID) and capillary column (SH-Stabilwax-DA). Phosphoric acid (30% wt.) was added to the samples before injecting to prevent the denaturation of some volatile acids. The nitrogen was used as the carrier gas with a flux of 4 mL/min. The temperature of the inject port and the detector were both maintained at 250°C. Elemental analysis of the hydrochar was carried out using Elementar Vario EL, and the elemental composition of feedstock is shown in Table 2. A scanning electron microscope (JSM 7800F Prime) was used to investigate the surface morphology features. The Raman measurements were performed on a customized Raman microscope equipped with a Pixis-100BR CCD (Princeton Instruments, USA), an Acton SP-2500i spectrograph, and a He Ne laser (14 mW). The surface functional groups of hydrochar were investigated using a Fourier transform infrared spectroscopy (FTIR) (PerkinElmer Spectrum Two, USA).

Table 2: Elemental composition and HHVs of the feedstock

Biowaste	Ultimate analysis (% dry wt.)					HHV (MJ/kg)
	C	N	H	S	O*	
Pine	42.87	1.52	6.14	0.07	44.50	17.48
Food waste	52.45	2.36	8.77	0.08	30.83	25.31
Sludge	18.10	3.26	3.07	0.05	19.47	6.70
<i>Chlorella vulgaris</i>	46.08	7.54	8.23	0.06	34.17	22.06

Note: *O% = 100% - C% - H% - N% - S% - Ash%. HHV = 0.3491 C + 1.1783 H - 0.1034 O + 0.1005 S - 0.0151 N - 0.0211 Ash.

3 Result and Discussion

3.1 Effects of Hydrochar on the Methane Production

The methane yield from anaerobic digestion with different hydrochar addition was presented in Fig. 1. As observed, the anaerobic digestion process was finished within approximately 40 h for all sets except for the F-C, and the methane yield of all groups reached a peak within 14~18 h. The total methane was only 218 mL for the F-C group, about two-thirds of the control group, while the cumulative methane volume of the S-C and P-C groups was close to that of the control group. This difference suggested that F-C addition was not favored for the anaerobic digestion process, and inhibiting effect can be seen during the initial stage (13~17 h). As for the C-C group, the total methane (about 345 mL) was higher than that of other groups, and a promotion effect on anaerobic digestion methanogenesis can be observed. There was a slight difference in methane production between the S-C, P-C group, and control groups. As a whole, with the same dose of hydrochar, methane volume was different, and it was speculated that F-C may not suitable for promoting methane production.

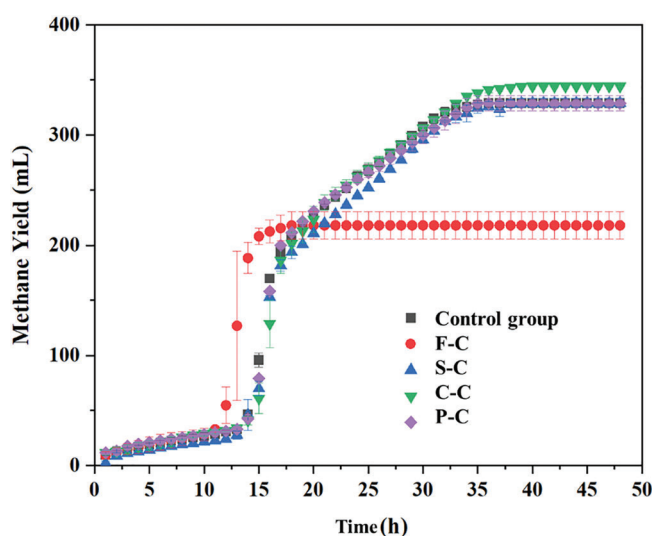


Figure 1: Methane production of food waste hydrochar (F-C), sludge hydrochar (S-C), *Chlorella* hydrochar (C-C), and pine hydrochar (P-C) assisted anaerobic digestion

3.2 Substrate Composition and Variation

To explore the effect of hydrochar on the metabolism of the organics, the TOC removal efficiency and variation of VAFs concentrations were investigated (Fig. 2). It can be observed that the TOC removal rate of the control, S-C, C-C, and P-C group on day-1 reached up to approximately 80%, indicating that most of the organics in the reaction system were consumed within 24 h, while the TOC completely consumed with 48 h. However, the TOC removal rate of substrate for F-C was only 51% on day-1, and this value increased by about 13% on day-2, which indicated 26% of organics still remained. Based on the VAFs analysis, a high content of VAFs 1.4 g/L was noticed on day-1, and this value increased to 1.6 g/L on day-2, so it can be speculated that the accumulation of VAFs aroused by F-C was the dominant reason for the low TOC removal. On the contrary, the addition of C-C showed the best result with the lowest VAFs on day-2. This comparison confirmed that F-C led to VAFs inhibition instead of a degradation promotion.

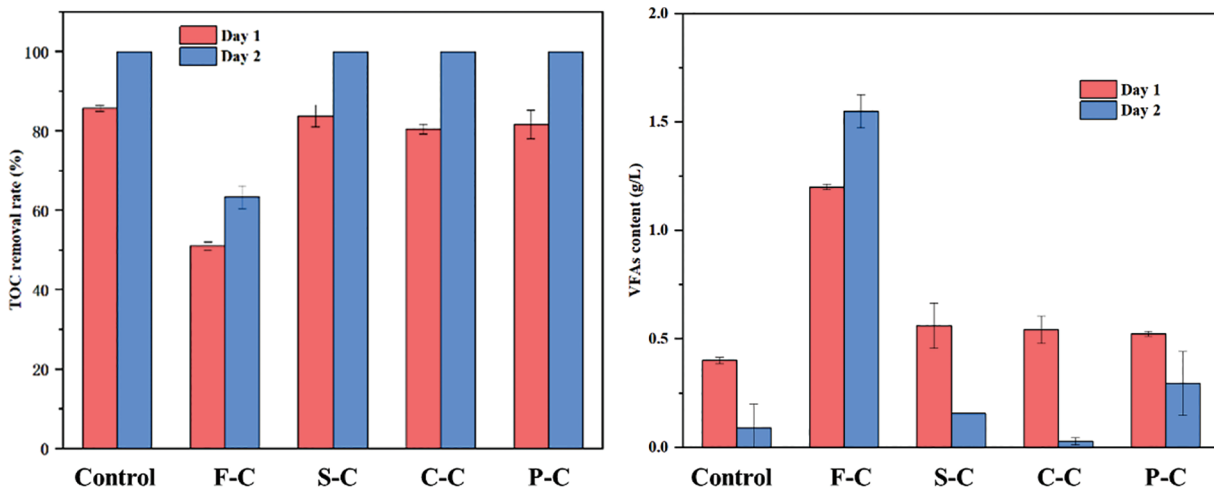


Figure 2: TOC removal and VFAs content of the substrate during AD on day-1 and day-2

Acetate, propionate, butyrate, pentanoate, and ethanol were the main products during acidification (Table 3). A higher distribution of VFAs and ethanol with hydrochar addition was observed. In particular, the much higher acetate, ethanol, and butyrate concentration in C-C, S-C and P-C group than that in the control group was observed. Combined with the similar TOC removal in C-C, S-C, and P-C groups and the control group, hydrochar derived from sludge, *Chlorella*, and pine may facilitate the VFAs and ethanol production from glucose compared to the control group. A similar result was also confirmed by Bu et al. [23] that biochar addition was assumed to promote acidification via enhancing electron transfer efficiency, stimulating bacterial growth, and improving critical enzymatic activities. It should be noted that F-C had the lowest TOC removal, relatively lowest acetate concentration 0.285, and higher butyrate 0.868 g/L on day 1. Tang et al. proposed the multiple roles of biochar in anaerobic digestion, including pH buffering, functional microbes enrichment, inhibitors alleviating, and regulating the hydrolysis, acidification, and methanogenesis [9]. It could be speculated that the F-C addition accelerated the acidification since the highest VFAs production on the day 1 (Table 3), compared to others. However, it inhibited acetogenesis and methanogenesis, and the methane production confirmed this in F-C group (Fig. 1), which suggested the shortest lag phase but the lowest methane production. It should be noted that all the hydrochar addition enhanced ethanol production. The ethanol could stimulate DIET's establishment by providing electrons and by enriching exoelectrogens and electrorophic methanogens for co-digesting complex organic wastes [24].

Table 3: Detailed VFAs and ethanol composition in the substrate on day-1

Sample	Acetate (g/L)	Propionate (g/L)	I-butyrate (g/L)	N-butyrate acid (g/L)	Pentanoate (g/L)	Ethanol (g/L)
Control	0.278 ± 0.012	0.036 ± 0.003	0.004 ± 0.002	0.071 ± 0.002	0.003 ± 0.001	0
F-C	0.285 ± 0.062	0.038 ± 0.036	0.009 ± 0.002	0.868 ± 0.055	0	0.018 ± 0.010
S-C	0.427 ± 0.075	0.043 ± 0.018	0.016 ± 0.001	0.114 ± 0.016	0	0.179 ± 0.028
C-C	0.307 ± 0.033	0.048 ± 0.017	0.013 ± 0.001	0.114 ± 0.003	0.012 ± 0	0.200 ± 0.056
P-C	0.308 ± 0.022	0.058 ± 0.006	0.019 ± 0.001	0.138 ± 0.027	0	0.160 ± 0.017

Accumulated VFAs in F-C assisted anaerobic digestion was found on the second day, and the concentration of acetate and butyrate reached up to 0.267 and 1.161 g/L, respectively, which were higher than that of other groups (Table 4). The accumulation of butyrate indicated the inhibition of methane production, and it can be observed that butyrate accounted for about 70% of the total VFAs for the F-C group. Acetate in the P-C group was completely consumed, indicating that the lignocellulose-derived hydrochar was favored for the acetotrophic methanogenesis, while the concentration of butyrate (0.398 g/L) was higher than that of S-C and C-C group. The low conductivity of F-C may account for the poor ability to develop DIET and enhance anaerobic digestion. In addition, food waste is known as a suitable feedstock for bio-oil production via hydrothermal conversion due to its high protein and lipid content. The produced F-C may mix with a small amount of bio-crude oil, which contains nitrogen heterocyclic and phenolic substances [25], and they would cause toxicity to the acetogens and methanogens, which further results in the accumulation of organic acids [26].

Table 4: Detailed VFAs and ethanol composition in the substrate on day-2

Sample	Acetate (g/L)	Propionate (g/L)	I-butyrate (g/L)	N-butyrate acid (g/L)	Pentanoate (g/L)	Ethanol (g/L)
Control	0.167 ± 0	0	0	0	0	0.008 ± 0.007
F-C	0.267 ± 0.013	0.062 ± 0.005	0.05 ± 0.007	1.161 ± 0.076	0.01 ± 0.001	0.013 ± 0.001
S-C	0.145 ± 0	0	0	0.01 ± 0	0	0.002 ± 0
C-C	0.195 ± 0.011	0	0	0	0	0.009 ± 0.001
P-C	0	0	0	0.398 ± 0	0	0.003 ± 0

3.3 Surface Functional Groups and Morphology Features

The surface functional groups in this work were analyzed by FTIR since oxygen-containing groups like C=O and -OH benefit the development of DIET [22]. As observed in Fig. 3, the 3600~3300 cm⁻¹ were assigned to overlapping peaks of hydroxyl and amino groups. This peak was more obvious for P-C, indicating that N-containing biowaste-derived hydrochar had limited oxygen groups [27]. All hydrochar consisted of distinct aliphatic methylene bands at 2925 and 2855 cm⁻¹, and it indicated the presence of aliphatic structures. The C=O stretching vibrational band of hemicellulose at 1730 cm⁻¹ suggested the presence of oxygen-containing functional groups on the surface of hydrochar [28]. This peak can be observed in all hydrochar except S-C, which may be attributed to the hemicellulose components, while sludge had a limited content of hemicellulose [29]. The peak at 1600 cm⁻¹ belonged to the aromatic C=C stretching in aromatic groups ascribed to the lignin content and this peak was more obvious in P-C than in other samples. The band around 1080 cm⁻¹ (1060–1260 cm⁻¹) was assigned to the C-O-C aliphatic ethers and C-O-C stretching in ether, and limited peaks in this range were found in S-C since ash dominated the main components in sludge instead of carbohydrate [30]. It can be concluded that all hydrochar preserved rich oxygen-containing groups like C=O and C-O, and it speculated that S-C and F-C had relatively low -OH due to the carbonization degree and ash content, respectively. Nevertheless, the nitrogen-containing components may not be the main reason for the difference in the electron transport of oxygen-containing functional groups, but the toxic substances contained in the hydrochar from F-C may account for this [31].

The surface morphological characteristics of all hydrochar samples are shown in Fig. 4. A large number of holes are generated on the surface of P-C, and the size of the particle is small. The microspheres are mainly formed by the carbonization of xylose and cellulose in pine [32]. Unlike lignocellulose from pine which undergoes the hydrolysis process, food waste can be easily carbonized and a large size (1~3 μm) of

hydrochar microspheres were formed. In contrast, few spherical particles and more irregular particles were observed for the S-C since its fixed carbon content was low. Thus, a porous structure on the surface of the hydrochar can be observed. However, algae hydrochar also had a large microsphere incorporated into the surface, which is different from that of F-C. No obvious relationship can be built between the surface morphological structure of hydrochars and methane production performance. It suggested that the main difference in methane production may not be attributed to hydrochar's surface morphological structure but the involvement and conductivity of toxic substances of hydrochar.

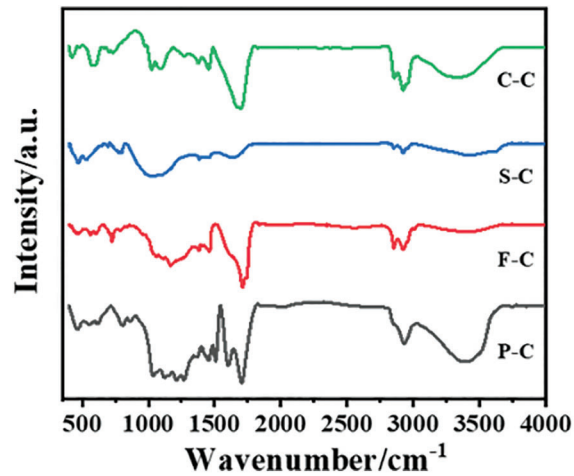


Figure 3: FTIR spectra of hydrochar prepared from four typical biowastes

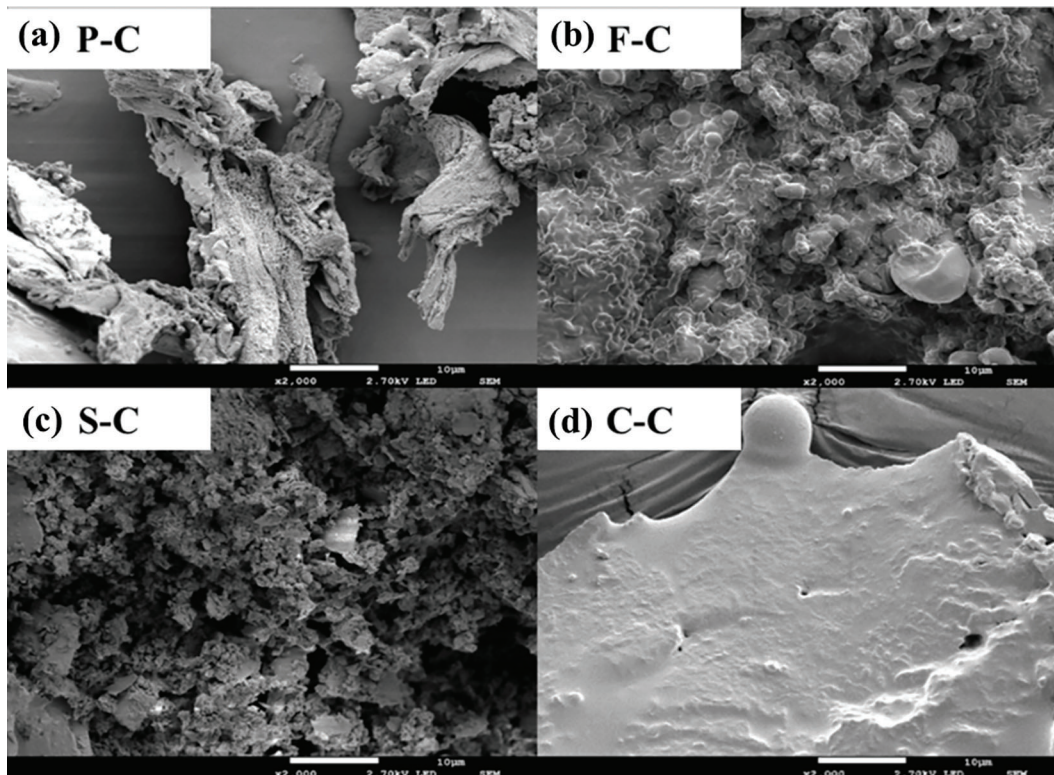


Figure 4: SEM images of hydrochar derived from different feedstock

3.4 The Elemental Composition and Carbonization Degree of Hydrochar

The carbon content in hydrochar increased from 42.87%–52.45% to 64.87%–72.64% in C-C, F-C, and P-C, except for S-C due to the ash content (Table 5). Especially the carbon content for F-C reached up to 72.64%, which suggested that F-C had a high carbonization degree coupled with the low O/C and H/C ratio. Additionally, it can be clearly seen that P-C had the highest oxygen content (25.17%). The carbon content for F-C reached 72.64%. As for N, the ratio in hydrochar was reduced from 1.52%–7.54% to 1.25%–6.45%, and P-C remained the lowest N content.

Table 5: Elemental analysis of hydrochar and model biowaste hydrochar

Hydrochar	C (%)	N (%)	H (%)	S (%)	*O (%)
P-C	64.87 ± 0.02	1.25 ± 0.03	5.27 ± 0.0005	0.029 ± 0.003	25.17 ± 0.07
F-C	72.64 ± 0.06	2.34 ± 0.04	5.24 ± 0.05	0.035 ± 0.002	18.95 ± 0.09
S-C	12.20 ± 0.05	1.33 ± 0.02	1.77 ± 0.04	0.034 ± 0.005	9.50 ± 0.11
C-C	67.91 ± 0.08	6.45 ± 0.02	6.69 ± 0.08	0.041 ± 0.003	15.23 ± 0.03

Note: *O% = 100%-C%-H%-N%-S%-Ash%.

Fig. 5 illustrates the Raman spectroscopy and the I_D/I_G value of hydrochar from different biowaste. The parameter of I_D/I_G can be used for the estimation of the graphitisation extent or graphite-like carbon structures in hydrochar [33]. As observed, C-C had the highest I_D/I_G value of 1.07, while the I_D/I_G value for S-C and F-C were 0.97 and 0.95, respectively. This suggested that C-C had the lowest degree of graphitization coupled with properly poor conductivity for the development of DIET, while the enhancement of biogas production may depend more on surface groups. The production of methane can also confirm this. However, P-C had the lowest I_D/I_G value (0.93). The high graphitization degree of P-C may be ascribed to the carbonization of components like cellulose and xylose by the formation of aromatic structures [34,35]. On the other hand, P-C was the only biowaste with low N content, and limited N can be incorporated into the matrix of carbon from hydrochar since it suggested that high temperature and Millard reaction can enhance the stable N forms formation like pyridine-N and quaternary-N, which can provide good conductivity for the hydrochar [36,37]. Based on this characteristic, it can be inferred that the DIET of pine-hydrochar in this work may rely more on the conductivity of body structure or physical structure rather than the surface oxygen-containing groups. Nevertheless, hydrochar from biowaste with rich nitrogen resources may depend more on the surface oxygen-containing groups due to the introduction of elemental N.

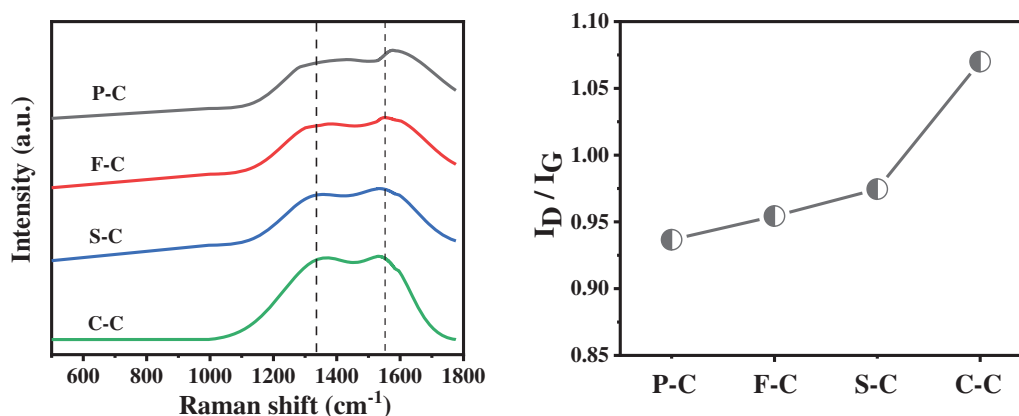


Figure 5: Raman spectroscopy and the I_D/I_G value of hydrochar

4 Conclusion

The present study suggested that hydrochar prepared with various biowastes had a significant difference during anaerobic digestion. Algae-derived hydrochar showed the best performance of methane production (about 345 mL) with high TOC removal efficiency. Nitrogen-containing biowaste hydrochar like C-C and S-C may build DIET. In comparison, F-C may produce toxic compounds and arouse severe acetate and butyrate accumulation. Unlike hydrochar obtained from N-containing biowaste, lignocellulose hydrochar like P-C may develop DIET by main pathways of the body with aromatic structure matrix. In general, hydrochar prepared from various biowaste can have a different effect on anaerobic digestion, and DIET may be established with diverse pathways according to the physicochemical characteristics of hydrochar.

Funding Statement: This work was financially supported by the Opening Project of Key Laboratory of Agricultural Renewable Resource Utilization Technology (No. HLJHDNY2104), Funding for the National Natural Science Foundation of China (NSFC U21A20162), Heilongjiang Postdoctoral Financial Assistance (LBH-Z21042), University Nursing Program for Young Scholars with Creative Talents in Heilongjiang Province (UNPYSCT-2020106), and Sichuan Science and Technology Program (2022NSFSC1162).

Conflicts of Interest: The authors declare that they have no conflicts of interest to report regarding the present study.

References

1. Duarah, P., Haldar, D., Patel, A. K., Dong, C. D., Singhanian, R. R. et al. (2022). A review on global perspectives of sustainable development in bioenergy generation. *Bioresource Technology*, 348, 126791. <https://doi.org/10.1016/j.biortech.2022.126791>
2. Shuba, E. S., Kifle, D. (2018). Microalgae to biofuels: 'Promising' alternative and renewable energy, review. *Renewable and Sustainable Energy Reviews*, 81, 743–755. <https://doi.org/10.1016/j.rser.2017.08.042>
3. Pocha, C. K. R., Chia, S. R., Chia, W. Y., Koyande, A. K., Nomanbhay, S. et al. (2022). Utilization of agricultural lignocellulosic wastes for biofuels and green diesel production. *Chemosphere*, 290, 133246. <https://doi.org/10.1016/j.chemosphere.2021.133246>
4. Scharlemann, J. P. W., Laurance, W. F. (2008). How green are biofuels? *Science*, 319(5859), 43–44. <https://doi.org/10.1126/science.1153103>
5. Li, G., Bai, X., Li, H., Lu, Z., Zhou, Y. et al. (2019). Nutrients removal and biomass production from anaerobic digested effluent by microalgae: A review. *International Journal of Agricultural and Biological Engineering*, 12(5), 8–13. <https://doi.org/10.25165/j.ijabe.20191205.3630>
6. Li, Y., Chen, Y., Wu, J. (2019). Enhancement of methane production in anaerobic digestion process: A review. *Applied Energy*, 240, 120–137. <https://doi.org/10.1016/j.apenergy.2019.01.243>
7. Sun, C., Xia, A., Liao, Q., Fu, Q., Huang, Y. et al. (2018). Improving production of volatile fatty acids and hydrogen from microalgae and rice residue: Effects of physicochemical characteristics and mix ratios. *Applied Energy*, 230, 1082–1092. <https://doi.org/10.1016/j.apenergy.2018.09.066>
8. Lee, J. Y., Park, J. H., Park, H. D. (2017). Effects of an applied voltage on direct interspecies electron transfer via conductive materials for methane production. *Waste Management*, 68, 165–172. <https://doi.org/10.1016/j.wasman.2017.07.025>
9. Tang, S., Wang, Z., Liu, Z., Zhang, Y., Si, B. (2020). The role of biochar to enhance anaerobic digestion: A review. *Journal of Renewable Materials*, 8(9), 1033–1052. <https://doi.org/10.32604/jrm.2020.011887>
10. Reguera, G., McCarthy, K. D., Mehta, T., Nicoll, J. S., Tuominen, M. T. et al. (2005). Extracellular electron transfer via microbial nanowires. *Nature*, 435, 1098–1101. <https://doi.org/10.1038/nature03661>
11. Zhao, Z., Li, Y., Zhang, Y., Lovley, D. R. (2020). Sparking anaerobic digestion: Promoting direct interspecies electron transfer to enhance methane production. *iScience*, 23(12), 101794. <https://doi.org/10.1016/j.isci.2020.101794>

12. Wang, Z., Wang, T., Si, B., Watson, J., Zhang, Y. (2021). Accelerating anaerobic digestion for methane production: Potential role of direct interspecies electron transfer. *Renewable and Sustainable Energy Reviews*, 145, 111069. <https://doi.org/10.1016/j.rser.2021.111069>
13. Capson-Tojo, G., Moscoviz, R., Ruiz, D., Santa-Catalina, G., Trably, E. et al. (2018). Addition of granular activated carbon and trace elements to favor volatile fatty acid consumption during anaerobic digestion of food waste. *Bioresource Technology*, 260, 157–168. <https://doi.org/10.1016/j.biortech.2018.03.097>
14. Wang, P., Peng, H., Adhikari, S., Higgins, B., Roy, P. et al. (2020). Enhancement of biogas production from wastewater sludge via anaerobic digestion assisted with biochar amendment. *Bioresource Technology*, 309, 123368. <https://doi.org/10.1016/j.biortech.2020.123368>
15. Wang, C., Wang, C., Jin, L., Lu, D., Chen, H. et al. (2019). Response of syntrophic aggregates to the magnetite loss in continuous anaerobic bioreactor. *Water Research*, 164, 114925. <https://doi.org/10.1016/j.watres.2019.114925>
16. Wang, Z., Zhang, C., Watson, J., Sharma, B. K., Si, B. et al. (2022). Adsorption or direct interspecies electron transfer? A comprehensive investigation of the role of biochar in anaerobic digestion of hydrothermal liquefaction aqueous phase. *Chemical Engineering Journal*, 435, 135078. <https://doi.org/10.1016/j.cej.2022.135078>
17. Yang, G., Zhang, Z., Kang, X., Li, L., Li, Y. et al. (2020). Fe-N-C composite catalyst derived from solid digestate for the oxygen reduction reaction in microbial fuel cells. *ACS Applied Energy Materials*, 3(12), 11929–11938. <https://doi.org/10.1021/acsaem.0c02072>
18. Usman, M., Shi, Z., Ren, S., Ngo, H. H., Luo, G. et al. (2020). Hydrochar promoted anaerobic digestion of hydrothermal liquefaction wastewater: Focusing on the organic degradation and microbial community. *Chemical Engineering Journal*, 399, 125766. <https://doi.org/10.1016/j.cej.2020.125766>
19. Wang, F., Wang, J., Li, Z., Zan, S., Du, M. (2020). Promoting anaerobic digestion by algae-based hydrochars in a continuous reactor. *Bioresource Technology*, 318, 124201. <https://doi.org/10.1016/j.biortech.2020.124201>
20. Falco, C., Baccile, N., Titirici, M. M. (2011). Morphological and structural differences between glucose, cellulose and lignocellulosic biomass derived hydrothermal carbons. *Green Chemistry*, 13, 3273–3281. <https://doi.org/10.1039/c1gc15742f>
21. Wang, T., Zhai, Y., Zhu, Y., Li, C., Zeng, G. (2018). A review of the hydrothermal carbonization of biomass waste for hydrochar formation: Process conditions, fundamentals, and physicochemical properties. *Renewable and Sustainable Energy Reviews*, 90, 223–247. <https://doi.org/10.1016/j.rser.2018.03.071>
22. Ren, S., Usman, M., Tsang, D. C. W., O-Thong, S., Angelidaki, I. et al. (2020). Hydrochar-facilitated anaerobic digestion: Evidence for direct interspecies electron transfer mediated through surface oxygen-containing functional groups. *Environmental Science & Technology*, 54(9), 5755–5766. <https://doi.org/10.1021/acs.est.0c00112>
23. Bu, J., Wei, H. L., Wang, Y. T., Cheng, J. R., Zhu, M. J. (2021). Biochar boosts dark fermentative H₂ production from sugarcane bagasse by selective enrichment/colonization of functional bacteria and enhancing extracellular electron transfer. *Water Research*, 202, 117440. <https://doi.org/10.1016/j.watres.2021.117440>
24. Feng, D., Guo, X., Lin, R., Xia, A., Huang, Y. et al. (2021). How can ethanol enhance direct interspecies electron transfer in anaerobic digestion? *Biotechnology Advances*, 52, 107812. <https://doi.org/10.1016/j.biotechadv.2021.107812>
25. Si, B., Watson, J., Aierzhati, A., Yang, L., Liu, Z. et al. (2019). Biohythane production of post-hydrothermal liquefaction wastewater: A comparison of two-stage fermentation and catalytic hydrothermal gasification. *Bioresource Technology*, 274, 335–342. <https://doi.org/10.1016/j.biortech.2018.11.095>
26. Reza, M. T., Andert, J., Wirth, B., Busch, D., Pielert, J. et al. (2014). Hydrothermal carbonization of biomass for energy and crop production. *Applied Bioenergy*, 1, 11–29. <https://doi.org/10.2478/apbi-2014-0001>
27. Wang, T., Zhai, Y., Zhu, Y., Peng, C., Xu, B. et al. (2018). Influence of temperature on nitrogen fate during hydrothermal carbonization of food waste. *Bioresource Technology*, 247, 182–189. <https://doi.org/10.1016/j.biortech.2017.09.076>
28. Sevilla, M., Fuertes, A. B. (2009). The production of carbon materials by hydrothermal carbonization of cellulose. *Carbon*, 47(9), 2281–2289. <https://doi.org/10.1016/j.carbon.2009.04.026>

29. Kang, S., Li, X., Fan, J., Chang, J. (2012). Characterization of hydrochars produced by hydrothermal carbonization of lignin, cellulose, d-xylose, and wood meal. *Industrial & Engineering Chemistry Research*, 51(26), 9023–9031. <https://doi.org/10.1021/ie300565d>
30. He, C., Zhang, Z., Ge, C., Liu, W., Tang, Y. et al. (2019). Synergistic effect of hydrothermal co-carbonization of sewage sludge with fruit and agricultural wastes on hydrochar fuel quality and combustion behavior. *Waste Management*, 100, 171–181. <https://doi.org/10.1016/j.wasman.2019.09.018>
31. Kruse, A., Koch, F., Stelzl, K., Wüst, D., Zeller, M. (2016). Fate of nitrogen during hydrothermal carbonization. *Energy and Fuels*, 30(10), 8037–8042. <https://doi.org/10.1021/acs.energyfuels.6b01312>
32. Titirici, M. M., Antonietti, M., Baccile, N. (2008). Hydrothermal carbon from biomass: A comparison of the local structure from poly- to monosaccharides and pentoses/hexoses. *Green Chemistry*, 10, 1204–1212. <https://doi.org/10.1039/b807009a>
33. Peng, C., Zhai, Y., Zhu, Y., Wang, T., Xu, B. et al. (2017). Investigation of the structure and reaction pathway of char obtained from sewage sludge with biomass wastes, using hydrothermal treatment. *Journal of Cleaner Production*, 166, 114–123. <https://doi.org/10.1016/j.jclepro.2017.07.108>
34. Brown, A. B., Tompsett, G. A., Partopour, B., Deskins, N. A., Timko, M. T. (2020). Hydrochar structural determination from artifact-free Raman analysis. *Carbon*, 167, 378–387. <https://doi.org/10.1016/j.carbon.2020.06.021>
35. Xiao, L. P., Shi, Z. J., Xu, F., Sun, R. C. (2012). Hydrothermal carbonization of lignocellulosic biomass. *Bioresource Technology*, 118, 619–623. <https://doi.org/10.1016/j.biortech.2012.05.060>
36. Falco, C., Sevilla, M., White, R. J., Rothe, R., Titirici, M. M. (2012). Renewable nitrogen-doped hydrothermal carbons derived from microalgae. *ChemSusChem*, 5(9), 1834–1840. <https://doi.org/10.1002/cssc.201200022>
37. Zhao, P., Chen, H., Ge, S., Yoshikawa, K. (2013). Effect of the hydrothermal pretreatment for the reduction of no emission from sewage sludge combustion. *Applied Energy*, 111, 199–205. <https://doi.org/10.1016/j.apenergy.2013.05.029>